

Serveur Académique Lausannois SERVAL serval.unil.ch

Author Manuscript

Faculty of Biology and Medicine Publication

This paper has been peer-reviewed but does not include the final publisher proof-corrections or journal pagination.

Published in final edited form as:

Title: Synaptic Adhesion Molecules Regulate the Integration of New Granule Neurons in the Postnatal Mouse Hippocampus and their Impact on Spatial Memory.

Authors: Krzisch M, Fülling C, Jabinet L, Armida J, Gebara E, Cassé F, Habbas S, Volterra A, Hornung JP, Toni N

Journal: Cerebral cortex (New York, N.Y. : 1991)

Year: 2016 Jul 29

DOI: [10.1093/cercor/bhw217](https://doi.org/10.1093/cercor/bhw217)

In the absence of a copyright statement, users should assume that standard copyright protection applies, unless the article contains an explicit statement to the contrary. In case of doubt, contact the journal publisher to verify the copyright status of an article.

Synaptic adhesion molecules regulate the integration of new granule neurons in the postnatal mouse hippocampus and their impact on spatial memory

Marine Krzisch, Christine Fülling, Laura Jabinet, Jan Armida, Elias Gebara, Frédéric Cassé, Samia Habbas, Andrea Volterra, Jean-Pierre Hornung, Nicolas Toni

Department of Fundamental Neurosciences, University of Lausanne, 9, rue du Bugnon, Lausanne, Switzerland

Running title: “Synaptic adhesion molecules in new neurons of postnatal hippocampus”

Correspondence should be addressed to:

Nicolas Toni

Department of Fundamental Neuroscience,
University of Lausanne,
9, rue du Bugnon, 1005 Lausanne, Switzerland.

Phone: +4121-692-5133

Fax: ++4121-692-5105

Email: Nicolas.toni@unil.ch

Abstract

Postnatal hippocampal neurogenesis induces network remodeling and may participate to mechanisms of learning. In turn, the maturation and survival of newborn neurons is regulated by their activity. Here, we tested the effect of a cell-autonomous overexpression of synaptic adhesion molecules on the maturation and survival of neurons born postnatally and on hippocampal-dependent memory performances.

Families of adhesion molecules are known to induce pre- and post-synaptic assembly. Using viral targeting, we overexpressed three different synaptic adhesion molecules, SynCAM1, Neuroligin-1B and Neuroligin-2A in newborn neurons in the dentate gyrus of 7- to 9-week-old mice. We found that SynCAM1 increased the morphological maturation of dendritic spines and mossy fiber terminals while Neuroligin-1B increased spine density. In contrast, Neuroligin-2A increased both spine density and size as well as GABAergic innervation and resulted in a drastic increase of neuronal survival. Surprisingly, despite increased neurogenesis, mice overexpressing Neuroligin-2A in new neurons showed decreased memory performances in a Morris water maze task.

These results indicate that the cell-autonomous overexpression of synaptic adhesion molecules can enhance different aspects of synapse formation on new neurons and increase their survival. Furthermore, they suggest that the mechanisms by which new neurons integrate in the postnatal hippocampus conditions their functional implication in learning and memory.

Introduction

In the mammalian brain, neurogenesis stops at birth except in the dentate gyrus of the hippocampus and the subventricular zone, where lifelong neurogenesis is commonly referred to as adult neurogenesis (Altman J and GD Das 1965; Eriksson PS et al. 1998). Although the function of adult neurogenesis in the hippocampus is debated (Jaholkowski P et al. 2009;

Groves JO et al. 2013; Lazic SE et al. 2014; Henn FA and B Vollmayr 2004), several lines of evidence indicate that the addition of new neurons enhances synaptic plasticity of the hippocampal network. Indeed, immature neurons display enhanced excitability and plasticity between 3 and 7 weeks after division (Schmidt-Hieber C et al. 2004; Ge S et al. 2007; Tronel S et al. 2010; Marin-Burgin A et al. 2012) and the experimental reduction of hippocampal adult neurogenesis in rodents results in learning and memory impairments (Saxe MD et al. 2006; Deng W et al. 2009). Notably, the optogenetic inhibition of new, still immature hippocampal granule neurons during a spatial memory recall task decreased performance (Gu Y et al. 2012), indicating that new neurons are directly involved in memory retrieval (Zhao C et al. 2008). Inversely, several studies show that improved learning and memory performances can be induced by increasing adult neurogenesis with enriched environment or voluntary exercise (Kempermann G et al. 1997; van Praag H et al. 1999) (but see Hauser T et al. 2009; Lazic SE et al. 2014), by the cell-autonomous inhibition of apoptosis in newly-formed neurons (Sahay A et al. 2011) or by the enhancement of neuronal fate differentiation (Richetin K et al. 2015).

The process of maturation and synaptic integration of new granule neurons varies greatly across species and lasts from about a month in rodents to several months in primates (Kohler SJ et al. 2011; Brus M et al. 2013). It follows distinct steps which are strongly activity-dependent: quickly after their differentiation, newborn neurons extend their axons to the CA3 region and their dendrites towards the molecular layer of the dentate gyrus. During this period, they receive functional GABAergic input (Song J et al. 2013) which, owing to a high chloride intracellular concentration, is depolarizing (Tozuka Y et al. 2005; Ge S et al. 2006). They also express N-methyl-D-aspartate receptors (NMDAr), but no α -amino-3 hydroxy-5-methyl-4-isoxazolepropionic acid receptors (AMPAr) and are therefore synaptically silent (Chancey JH et al. 2013). The concurrent GABA_A receptor-mediated depolarization and

glutamate-mediated NMDAr activation lead to the expression of AMPAr at the post-synaptic membrane, thereby unsilencing the activated neurons (Chancey JH et al. 2013). This stage is required for the formation of dendritic spines, since interfering with GABA_A-mediated depolarization or D-serine availability, a NMDAr co-agonist, result in impaired dendritic development and synaptic integration (Ge S *et al.* 2006; Sultan S et al. 2015). Upon formation, immature dendritic spines preferentially contact pre-existing axon terminals already synapsing with one or several postsynaptic granule neurons and thereby form multiple synapse boutons (MSB); (Toni N et al. 2007). The consequent transformation of MSB into single synapse boutons suggests that dendritic spines from new neurons compete with spines from more mature neurons (Toni N *et al.* 2007; Toni N and S Sultan 2011; Bergami M and B Berninger 2012). Concomitantly, the majority of postnatally-born neurons die during the first month of maturation (Kempermann G et al. 2003) and a drastic elimination of new neurons occurs during the first steps of glutamatergic synaptogenesis, during the third week of maturation (Tashiro A et al. 2007). Furthermore, knocking out the essential NMDAr subunit NR1 specifically in newborn neurons drastically reduces their survival. This effect can be mitigated by the inhibition of overall NMDAr activity with the NMDAr selective antagonist 3-(2-Carboxypiperazin-4-yl)propyl-1-phosphonic acid (CPP) during the critical phase of maturation (Tashiro A et al. 2006). Together, these results suggest that the competitive process of synapse formation and stability plays a crucial role in the survival of newborn neurons. It is therefore possible that manipulations aimed at increasing synapse formation specifically on new neurons may improve their survival during this critical phase. In turn, these manipulations may result in improved hippocampal-dependent memory performances. To directly test this possibility, we used a viral-mediated gene transfer approach to increase the expression of synaptic adhesion molecules specifically in new granule, hippocampal neurons, in 7- to 9- week-old mice. In the context of synaptic competition between immature

and mature neurons, the use of a retroviral approach is crucial, since it enables to test the cell-autonomous effect of an increase in synapse formation on the integration of a subset of newborn neurons, without interfering with the mature neuronal network into which they integrate.

Several adhesion molecules enable pre- and post-synaptic assembly. These proteins include neurexins/neuroligins and the SynCAM proteins of the immunoglobulin superfamily (Biederer T and M Stagi 2008; Jin Y and CC Garner 2008; Giagtzoglou N et al. 2009). Interestingly, the expression of these molecules in non-neuronal cells enables synapse formation with co-cultured neurons, indicating that they have strong synaptogenic properties (Scheiffele P et al. 2000; Biederer T et al. 2002; Graf ER et al. 2004). We overexpressed three different synaptic adhesion molecules in new granule neurons: SynCAM1, Neuroigin-1B (NL1B) and Neuroigin-2A (NL2A). These molecules were chosen for their distinct and complementary roles: SynCAM1 is a transmembrane protein located pre- and post-synaptically, that engages in hetero- and homophilic adhesive interactions. In neurons, SynCAM1 overexpression increases excitatory synapse number, whereas the loss of SynCAM1 or the overexpression of its cytosolic domain (ctSynCAM1), acting as a dominant negative form of SynCAM1, result in fewer synapses (Biederer T *et al.* 2002). Neuroligins are transmembrane proteins located post-synaptically, and act as ligands for presynaptic neurexins (Ichtchenko K et al. 1995; Nguyen T and TC Sudhof 1997; Boucard AA et al. 2005; Comoletti D et al. 2006; Craig AM and Y Kang 2007). Similarly to SynCAM, Neuroligins mediate the formation and maintenance of synapses between neurons *in vitro* and *in vivo* (Scheiffele P *et al.* 2000; Graf ER *et al.* 2004; Prange O et al. 2004; Kwon HB et al. 2012; Zeidan A and NE Ziv 2012) and are involved in the formation of excitatory synapses (Budreck EC et al. 2013). There are several isoforms and splice variants of Neuroligins with different roles in specific synapse formation (Nguyen T and TC Sudhof 1997; Chih B et al.

2005; Varoqueaux F et al. 2006) and Neuroligin-1B (NL1B) overexpression increases glutamatergic synaptogenesis in cultured hippocampal neurons (Chih B *et al.* 2005). NL1 is only present at excitatory synapses (Song JY et al. 1999) whereas Neuroligin-2 (NL2) is present at inhibitory synapses (Varoqueaux F et al. 2004; Hoon M et al. 2011). NL2A overexpression in hippocampal neurons induces both glutamatergic and GABAergic synapse formation (Chih B et al. 2006).

These molecules were co-expressed with a fluorescent reporter to enable the identification of the targeted neurons and enable the assessment of their maturation and survival. We found that SynCAM1 and Neuroligin-1B overexpression had significant but subtle effects on the synaptogenesis of new neurons and did not modify their survival. In contrast, NL2A overexpression significantly increased both the glutamatergic and GABAergic inputs on new neurons and increased their survival. However, despite increased neurogenesis, mice with NL2A overexpressing new hippocampal neurons displayed impaired spatial memory performances.

Materials and Methods

Experimental animals

The animals used in this study were 7- to 9-week-old C57BL/6-J male mice. Mice were group-housed in standard cages under light- (12 h light/dark cycle) and temperature-controlled (22°C) conditions. The maximal number of mice per cage was 5. Food and water were available *ad libitum*. Every effort was made to minimize the number of animals used and their suffering. Experimental protocols were approved by the Swiss animal experimentation authorities.

Virus-mediated gene expression

To selectively express the genes of interest in new hippocampal neurons, we used Moloney murine leukemia viruses (MoMuLV) as previously described (Zhao C et al. 2006). Final virus titers were 10^7 - 10^8 particles forming unit/milliliter (pfu/mL) and 2 μ L of the mix were injected into each of the two dentate gyri at the following coordinates from the Bregma: anteroposterior -2 mm, lateral +1.75 or -1.75 mm and dorso-ventral -2.25 mm. After every injection and throughout the experiment, animals were regularly monitored for their physical recovery.

To test proper expression and localization of the gene of interest, Human embryonic kidney (HEK) 293T cells were infected with 10^4 pfu of retrovirus carrying each construct (1 μ L), and immunohistochemistry and immunoblotting against the corresponding adhesion molecule was performed. Expression of the proteins was effective and localized at the cell plasma membrane (SynCAM1, NL1B, NL2A) or in the cytosol (SynCAM1 cytosolic tail), showing proper addressing of the proteins after synthesis (Supplementary Figure 1).

Brain slice preparation and immunohistochemistry

Mice were perfused with 4% paraformaldehyde in phosphate buffered saline, their brains were cryoprotected and sectioned at a thickness of 60 μ m. RFP signal was amplified using rabbit anti-RFP IgG (600-401-379 Rockland Immunochemicals, Gilbertsville, Pennsylvania, USA; 1:1000) and Hylite 594 goat anti-rabbit IgG secondary antibody (61056-1-H594 Anawa trading SA, Wangen, Switzerland; 1:500). GFP signal was amplified using Chicken anti-GFP IgG (GFP-1020 Aves Labs, Tigard, Oregon, USA; 1:1000) and Dylight 488 goat anti-chicken IgY (603-141-126 Anawa Trading SA; 1:500). Vesicular GABA Transporter (VGAT) was detected using mouse anti-VGAT IgG (131011 Synaptic Systems GmbH, Goettingen, Germany; 1:1000) and Hylite 594 goat anti-mouse IgG secondary antibody (61057-05-H594 Anawa trading SA; 1:500). GABA_A receptors were detected using rabbit anti-GABA_A

receptor IgG (AGA-001 Alomone Labs, Jerusalem, Israel; 1:500) and donkey Dylight 649 anti-rabbit IgG secondary antibody (611-743-127 Anawa trading SA; 1:500). Arc was detected using rabbit anti-Arc IgG (156003 Synaptic systems; 1:500) and donkey Dylight 649 anti-rabbit IgG secondary antibody (611-743-127 Anawa trading SA; 1:500).

In HEK 293T cells cultures infected with MoMuLVs, SynCAM1 was detected using chicken anti-SynCAM IgG (CM004-3 MBL International, Woburn, MA, USA; 1:1000) and Dylight 488 goat anti-chicken IgY (603-141-126 Anawa Trading SA; 1:500). ctSynCAM1 was detected using rabbit anti-SynCAM1 IgG (S 4945, Sigma-Aldrich Chemie GmbH, Buchs, Switzerland; 1:5000) and Cy3 goat anti-rabbit IgG secondary antibody (111-165-144, Jackson ImmunoResearch Laboratories, Westgrove, PA, USA; 1:500). NL1B was detected using goat anti-Neurologin-1 IgG (ANR-036; Alomone labs; 1:25) and donkey Alexa 555 anti-goat IgG secondary antibody (A21432 Invitrogen, Lucerne, Switzerland; 1:250). NL2A was detected using rabbit anti-Neurologin-2 IgG (sc-50394 Santa Cruz biotechnologies; 1:100) and goat Hylite 594 anti-rabbit IgG secondary antibody (61056-1-H594 Anawa trading SA; 1:500). 4,6 Diamidino-2-phenylindole (DAPI) was used to reveal nuclei.

Confocal microscopy and image analyses

Hippocampal sections were imaged using a Zeiss LSM 710 confocal microscope (Carl Zeiss, Feldbach, Switzerland). Global views of neurons were imaged with a 40x oil lens and a z-step of 2 μm , and dendrites or mossy fiber terminals (MFT) were imaged with a 63x oil lens and a z-step of 0.38 μm . To assess GABAergic synapse density, dendrites were imaged with a 40x oil lens and a z-step of 0.45 μm . To measure differences in axonal length between ctSynCAM1-expressing and control neurons, the beginning and the end of the CA3 area were imaged using a 40x oil lens and a z-step of 2 μm . All analyses were performed using Fiji software (freely available at <http://fiji.sc/>).

Dendritic spine density was defined as the number of spines divided by the length of the dendritic segment. Dendritic spine density and diameter were measured on maximal intensity projections. Protrusions with a diameter inferior to 0.3 μm were considered as filopodia, with a diameter comprised between 0.30 μm and 0.55 μm as thin spines and protrusions with a diameter greater than 0.55 μm as mushroom spines. GABAergic synapses were defined as appositions of vesicular GABA transporter (VGAT)-positive and GABA_A receptor (GABA_AR)-positive puncta after immunohistochemistry against VGAT and GABA_AR. GABAergic synapse density was analyzed on individual optical sections of confocal z-stacks and measured as the number of GABAergic synapses divided by the length of the dendritic segment.

The maturation of MFT was evaluated by measuring their area, perimeter, number of extensions and circularity, defined as $4 \times \pi \times \text{area} / (\text{perimeter})^2$. The area and perimeter of MFT were measured on maximal intensity projections by tracing the contour of the MFT, excluding the satellites and filopodia. The number of extensions of the MFT was defined as the number of filopodia or satellites starting at the core of the MFT. Branching of satellites was not included in the counting (Figure 1J).

Sholl analysis was performed on maximal intensity projections. Since neurons from different parts of the dentate gyrus had a different maximal length, the space between each radius was set up at 10% of the maximal length of the neuron (Krzisch M et al. 2013).

Maximal dendritic extension was measured on maximal intensity projections and was defined as the ratio between the distance from the soma to the tip of its longest dendrite and the distance from the soma to the end of the molecular layer of the dentate gyrus (Krzisch M *et al.* 2013).

The survival of new neurons was assessed by injecting 8 mice with the same mixture of retroviruses, and analyzing 4 mice at 14 days post injection (dpi) and 4 mice at 28 dpi. For

each mouse, the ratio between the total number of overexpressing neurons and the total number of control neurons was calculated at the two timepoints. An increased ratio indicated increased survival of neurons overexpressing the protein of interest (Figure 10); (Tashiro A *et al.* 2006).

To compare the neuronal activity of control and overexpressing neurons, retrovirus injected mice were placed in environmental enrichment for 10 minutes. 30 to 90 minutes after enrichment, mice were sacrificed. One hundred neurons of each group were analyzed per mouse, and the proportion of new neurons that expressed the immediate-early gene Arc was calculated for control and overexpressing neurons in each mouse.

Behavioral tests

Elevated plus maze

Anxiety-like behavior was assessed with the elevated plus maze (EPM). The EPM consists of two open and two enclosed arms (30.5 x 5.5 cm) emanating from a central platform (5.5x5.5 cm). Mice were placed in the center of the maze facing a closed arm and allowed to freely explore the maze for 5 min. Animals' behavior was recorded and analyzed using ANY-maze software (Stoelting).

Morris water maze

Spatial learning and memory was assessed using the Morris water maze at 28 dpi. Behavioral testing was conducted in a dimly lit room (30 lx at the rim of the water). The water maze pool (Ø 140 cm) was filled with 20 cm water (25 °C) made opaque by adding 200 ml of milk. An escape platform (Ø 12 cm) was submerged 1 cm below the water surface in the east quadrant (target quadrant) of the pool. To facilitate the animals' orientation five distinct cues were glued inside of the pool approximately 20 cm above water level. Water maze training took place across seven consecutive days for four trials/day per animal

with an inter trial interval of 15 s. A trial was completed when the animal climbed on the platform or 40 s had elapsed. Upon failure to find the target platform during training, animals were guided to the target platform and left there for 10 s. Following training, spatial memory was assessed by two probe trials, conducted at 24 h and 120 h after last training session. Opposite starting positions were used for each probe trial. During probe trial sessions, the platform was removed from the pool and animals were left to swim for 40 s. The latency to find the platform during training sessions as well as the time animals spend in each quadrant during the probe test was analyzed using ANY-maze software (Stoelting).

Immunoblotting

Transfected HEK 293T cells were homogenized in ice-cold lysis buffer (15 mM Tris-HCl, pH 7.6, 320 mM sucrose, 1 mM DTT, 1 mM MgCl₂, 3 mM EDTA-K, 0.5% protease inhibitor cocktail (Sigma, P8340), 1% phosphatase inhibitor cocktail 1 (Sigma, P2850), and 1% phosphatase inhibitor cocktail 2 (Sigma, P5726). Protein samples were sonicated and frozen at -80 °C. Protein extracts (10 mg) were run on 10% SDS-PAGE by application of 110 volts for 90 min. After running, proteins were transferred on nitrocellulose membranes (84261514; Whatman) by application of 375 mA for 90 min at 4 °C. Then, membranes were incubated in the Odyssey blocking buffer (927-40000; LI-COR) at room temperature for 1 h and then incubated overnight at 4 °C with the following primary antibodies : mouse anti-RFP (RF5F, ThermoFisher scientific, 1/1000), rabbit anti-GFP (A-11122, ThermoFisher scientific, 1/1000), rabbit anti-SynCAM1 (S 4945, Sigma-Aldrich, 1:1000), goat anti-Neuroigin-1 (Alomone labs; 1:250), rabbit anti-Neuroigin-2 (Santa Cruz biotechnologies; 1/500). After washes in Phosphate Buffer Saline (PBS), secondary antibodies anti-mouse IgG IRDye 800 (1:10000, 610-132-121; Bioconcept), anti-rabbit IgG Alexafluor 680 (1:10000, Juro, Lucerne, Switzerland) and anti-goat IgG Alexafluor 680 (1:10000, Juro, Lucerne,

Switzerland) were applied for 1 h at room temperature and protected from light. After washing with PBS, membranes were scanned with the ODYSSEY Infrared Imaging System (LI-COR Biosciences).

Statistical analyses

Hypothesis testing was two-tailed. All analyses were performed using GraphPad Prism 6 (Graphpad Software, Inc., La Jolla, California, USA). First, Shapiro-Wilk tests were performed on each group of data to test for distribution normality. When the distribution was not normal, the non-parametric Mann-Whitney test was applied. When the distribution was normal, the equality of variances of the groups was tested and the adequate unpaired t-test was used. Data are presented as mean \pm SEM. For Sholl analyses, the total dendritic length of control and overexpressing neurons was calculated and used for statistical analyses. Two-way repeated measure ANOVA was used to compare treatment groups in the Morris water maze and one sample t-test was applied to estimate whether % time spent in the target quadrant during the probe trial was significantly different from 25 %.

Results

ctSynCAM1 decreases the synaptic maturation and survival of new neurons

To investigate whether SynCAM1 is involved in the synaptic integration of new neurons, we overexpressed ctSynCAM1 and the green fluorescent protein (GFP) in new hippocampal neurons using a retroviral vector derived from the Moloney murine leukemia virus (MoMuLV, Zhao C *et al.* 2006). ctSynCAM1 contains the full length cytoplasmic tail of SynCAM1, so cannot engage in adhesive interactions. It therefore acts as a competitive inhibitor of endogenous SynCAM1. The same viral vector enabling the expression of the red fluorescent protein (mRFP1) alone was co-injected as a control, to enable the identification of

wild-type new neurons in the same mice (Supplementary Figure 1A). *In vitro* infection of HEK 293T cells with the vector encoding ctSynCAM1 resulted in strong cytoplasmic expression of GFP and membrane expression of ctSynCAM1, as observed by immunohistochemistry and Western blot (Supplementary Figure 1B-C).

Both viral vectors were then injected in the dentate gyrus of 7- to 9-week-old mice and, 14, 21 or 28 days later (days post-injection, dpi), labeled new neurons were observed using confocal microscopy (Figure 1A). We first assessed the development of their dendritic branching using Sholl analysis. The number of branches was transiently increased by ctSynCAM1 expression at 21 dpi, but not at 14 or 28 dpi (Mann-Whitney test on the total dendritic length, 14 dpi: $p>0.05$; 21 dpi: $p=0.002$; 28 dpi: $p>0.05$; Supplementary Figure 2A), suggesting a role of SynCAM1 in dendritic maturation.

The vast majority of dendritic protrusions bear glutamatergic synapses and appear during the third week after cell division (Zhao C *et al.* 2006; Toni N *et al.* 2007). To assess the development of glutamatergic input on new neurons, we measured the density of dendritic protrusions at 21 and 28 dpi. The density of dendritic protrusions was not modified at 21 and 28 dpi in both the first third of the molecular layer (ML, principally innervated by commissural/associative afferences, 21 dpi: $p>0.05$; 28 dpi: $p>0.05$; Figure 1A, B) and the middle third of the ML (innervated by perforant path afferences from the entorhinal cortex, 21 and 28 dpi: $p>0.05$; Figure 1A, C).

The maturation of dendritic protrusions is characterized by an increase in diameter of the protrusions' tip (Zhao C *et al.* 2006; Toni N *et al.* 2007), reflecting the expression of AMPA receptors and synapse unsilencing (Takumi Y *et al.* 1999; Matsuzaki M *et al.* 2001). To examine whether ctSynCAM interfered with the maturation of dendritic protrusions, we measured the diameter of the tip of dendritic protrusions. Protrusions with a diameter inferior to 0.3 μm were considered as filopodia, with a diameter comprised between 0.30 μm and 0.55

μm as thin spines and protrusions with a diameter greater than $0.55 \mu\text{m}$ as mushroom spines (Figure 1D); (Sultan S et al. 2013). At 21 and 28 dpi, the proportion of mushroom spines was decreased and the proportion of filopodia and thin spines was increased by ctSynCAM1 expression (filopodia: 21 dpi: $p=0.017$; 28 dpi: $p=0.001$; thin: 21 dpi: $p>0.05$; 28 dpi: $p=0.0001$; mushroom: 21 dpi: $p=0.0003$; 28 dpi: $p<0.0001$; Figure 1E-F), indicating that interfering with SynCAM1 altered the maturation of dendritic protrusions on new neurons.

We next examined the effect of ctSynCAM1 expression on the axonal maturation of new neurons. The main efferences from new granule neurons are mossy fibers, with terminals (MFT) synapsing on dendrites of CA3 area pyramidal neurons. With maturation, there is an increase in the length of mossy fiber axons and of MFT surface area, perimeter and number of extensions protruding from MFT and a decrease in circularity (Zhao C et al. 2006; Toni N et al. 2008). New neurons expressing ctSynCAM1 displayed reduced morphological maturation of MFT at 28 dpi (area: $p=0.02$; perimeter: $p=0.007$; circularity: $p=0.04$; number of extensions: $p=0.003$; Figure 1I-N). Thus ctSynCAM1 expression also reduced the axonal maturation of new neurons.

Finally, we examined whether the decreased maturation of dendritic protrusions and MFT was associated with changes in neuronal survival. Survival between 14 and 28 dpi was assessed by injecting mice with the same mixture of ctSynCAM and control virus and comparing the ratio of ctSynCAM1-expressing over control neurons at both time points (Figure 1O); (Tashiro A et al. 2006). The ratio between ctSynCAM1-expressing and control new neurons decreased between 14 and 28 dpi, indicating that ctSynCAM1 expression decreased new neuron survival ($p=0.04$; Figure 1P).

Together, these results indicate that ctSynCAM1 interferes with the pre- and post-synaptic maturation as well as with the survival of newborn neurons. We therefore assessed whether

synCAM1 overexpression in new neurons was sufficient to enhance their synaptic integration and survival.

SynCAM1 overexpression increases presynaptic maturation but not the survival of new neurons

To enable the overexpression of SynCAM1 in a cohort of new neurons, we engineered the MoMuLV retroviral vector to express SynCAM1 and mRFP1. A retroviral vector encoding for GFP was used as a control. Membrane expression of SynCAM1 on HEK 293T cells was confirmed by immunohistochemistry and Western blot (Supplementary Figure 1B-C). Both viral vectors were then injected in the dentate gyrus and new neurons were examined using confocal microscopy. At 21 and 28 dpi, SynCAM1 overexpression did not affect dendritic tree complexity (21 dpi: $p > 0.05$; 28 dpi: $p > 0.05$; Supplementary Figure 2B) or spine density (first third of the ML: 21 dpi: $p > 0.05$; 28 dpi: $p > 0.05$; second third of the ML: 21 dpi: $p > 0.05$; 28 dpi: $p > 0.05$; Figure 1 B-C). At 28 dpi however, SynCAM1 overexpression increased the proportion of mushroom spines and decreased the proportion of thin spines and filopodia (filopodia: $p < 0.0001$; thin: $p < 0.0001$; mushroom: $p = 0.003$; Figure 1 G-H). SynCAM1 overexpression also increased MFT area and perimeter at 28 dpi (area: $p = 0.01$; perimeter: $p = 0.007$; Figure 1I-N). Thus SynCAM1 overexpression increased the presynaptic and postsynaptic maturation of new neurons.

We next assessed whether SynCAM1 overexpression increased the survival of new neurons by co-injecting SynCAM1-GFP and RFP control viruses. The ratio of SynCAM1-overexpressing and control neurons was similar at 14 dpi and 28 dpi ($p > 0.05$; Figure 1Q), indicating that SynCAM1 overexpression did not modify the survival of new neurons.

Together, these results indicate that SynCAM1 plays a role in the pre- and postsynaptic maturation of new neurons as well as in their survival. However, the overexpression of SynCAM1 was not sufficient to increase new neurons' survival.

Neuroigin-1B overexpression increases dendritic spine density but not the survival of new neurons

We next assessed the effect of NL1B overexpression on the synaptic integration of new neurons. To this aim, we engineered the MoMuLV viral vector to enable the co-expression of NL1B and GFP and a virus enabling the expression of mRFP1 was used as a control. The specificity and efficiency of transgene expression was controlled on HEK 293T cells by immunohistochemistry and Western blot (Supplementary Figure 1B-C).

On new granule neurons, NL1B overexpression did not modify dendritic tree complexity (14 dpi: $p>0.05$; 21 dpi: $p>0.05$; 28 dpi: $p>0.05$; Supplementary Figure 2C), but increased the density of dendritic protrusions in the second third of the ML at 21 and 28 dpi, but not in the first third of the ML (first third of the ML: 21 and 28 dpi: $p>0.05$; second third of the ML: 21 dpi: $p=0.04$; 28 dpi: $p=0.02$; Figure 2A-C).

In contrast to SynCAM1, NL1B overexpression did not affect the diameter of dendritic protrusions ($p>0.05$; Figure 2D, E) or the MFT area, perimeter, circularity, or number of extensions at 28 dpi ($p>0.05$; Figure 2F-I). Finally, we measured the survival of NL1B-overexpressing new neurons between 14 and 28 dpi. The proportion of NL1B-overexpressing relative to mRFP1-expressing control newborn neurons did not change between 14 and 28 dpi ($p>0.05$; Figure 2J), indicating that survival was not modified by NL1B overexpression.

Together, these results indicate that NL1B overexpression in newborn neurons slightly increased the density of dendritic protrusions but did not modify their maturation, the maturation of MFT, nor the survival of newborn neurons.

Neuroigin-2A overexpression increases glutamatergic and GABAergic synapses on newborn neurons, as well as their survival

Given the critical role of GABAergic input on the development of new neurons (Tozuka Y *et al.* 2005; Ge S *et al.* 2006), we hypothesized that NL2A overexpression may have a greater effect on new neuron maturation than NL1B or SynCAM1. To test this possibility, we injected mice with a MoMuLV viral vector encoding GFP and NL2A and a control vector encoding mRFP1 (Supplementary Figure 1). NL2A overexpression transiently increased dendritic tree complexity at 14 dpi, but not at later time points (14 dpi: $p=0.009$; 21 and 28 dpi: $p>0.05$; Supplementary Figure 2). Furthermore, NL2A increased the density of dendritic protrusions in the first and second third of the ML at 21 dpi and in the first third of the ML at 28 dpi (first third: 21 dpi: $p<0.0001$; 28 dpi: $p=0.001$; second third: 21 dpi: $p=0.02$; 28 dpi: $p>0.05$; Figure 3A-B). Furthermore, in the second third of the ML the proportion of filopodia was reduced at 28 dpi (21 dpi: $p>0.05$; 28 dpi: $p=0.009$; Figure 3C-E). These results indicate that NL2A increased the number and maturation of glutamatergic synaptic inputs on new neurons. We next assessed the effect of NL2A overexpression on the maturation of MFT. At 28 dpi, NL2A overexpression increased MFT area, but did not modify MFT perimeter, number of extensions and circularity (area: $p=0.005$; perimeter: $p>0.05$; circularity: $p>0.05$; number of extensions: $p>0.05$; Figure 3F-I). We then assessed the effect of NL2A overexpression on the density of inhibitory synapses on new neurons, using VGAT- and GABA_A receptor immunostaining. We quantified the density of appositions of VGAT-positive and GABA_AR-positive puncta on the soma and proximal dendrites of new neurons. GABAergic synapse density was increased on NL2A-overexpressing neurons (soma: $p=0.009$; proximal dendrite: $p=0.03$; Figure 3J-L). Thus, consistent with a role of NL2A in both glutamatergic and GABAergic synapse formation, the overexpression of this adhesion

molecule on newborn neurons increased the density of glutamatergic and GABAergic synaptic inputs, without modifying their output synapses.

We then assessed the effect of NL2A overexpression on the survival of new neurons. NL2A overexpression increased survival between 14 and 28 dpi by 3 fold ($p=0.03$; Figure 3M). The increased number of glutamatergic and GABAergic synapses on new neurons may result in changes in the activity of the targeted new neurons. To assess the recruitment of NL2A-overexpressing new neurons in network activity, we examined the expression of the immediate-early gene activity-regulated cytoskeleton-associated protein (Arc) in mice living in an enriched environment. Mice were virally injected and, 28 days later, were placed into an enriched environment for 10 minutes and sacrificed 30 to 90 minutes later. The ratio between the number of newborn neurons expressing Arc and the total number of newborn neurons was measured for NL2A-overexpressing and control newborn neurons. NL2A-overexpressing new neurons expressed Arc significantly more frequently than control new neurons ($p=0.02$; Figure 3N).

Together, these results indicate that NL2A overexpression in new neurons increased their synaptic integration and survival and enhanced their recruitment in network activity.

Neuroigin-2A overexpression in newborn neurons decreases spatial learning performances

Between 3-7 weeks after division, newborn neurons display increased plasticity and are preferentially recruited in learning tasks (Schmidt-Hieber C *et al.* 2004; Ge S *et al.* 2007; Gu Y *et al.* 2012). Since NL2A induced an increase in newborn neurons integration and survival during this period, we hypothesized that NL2A overexpression in newborn neurons may modify the animals' performances in spatial learning and memory tasks. To test this possibility, we assessed the behavior of mice injected with NL2A-overexpressing or GFP-

expressing MoMulV (Figure 4A). At 24 dpi, mice were first tested on an elevated plus maze, to assess anxiety. There was no intergroup difference in time spent in the open arm maze ($p > 0.05$, data not shown), indicating that anxiety level was similar between groups. At 28 dpi, mice were trained in a Morris water maze, in a fixed platform task for 7 days. There was no inter-group difference in swim speed ($p > 0.05$, data not shown) and distance traveled ($p > 0.05$, data not shown), indicating no difference in locomotion. During the training sessions, escape latencies were not significantly different between groups (two-way repeated measure ANOVA; main effect of time $F(6,162)=22.53$, $p < 0.0001$; main effect of treatment $F(6,162)=3.67$, $p > 0.5$; Figure 4B), indicating that learning performances were similar between groups. Twenty-four and 120 hours after the last training session (i.e. at 35 and 39 dpi), memory was tested with a probe trial (Figure 4A). Twenty-four hours after the last training session (probe 1), both groups of mice displayed a preference for the target quadrant (two-way repeated measure ANOVA, main effect of % time in quadrant $F(3,81)=31.27$, $p < 0.0001$, Bonferroni post-hoc tests target quadrant vs. opposite for both groups $p < 0.01$, target vs left quadrant $p < 0.01$, target vs right quadrant for GFP $p < 0.001$ NL2A $p > 0.05$) and the proportion of total time spent in the target quadrant was significantly above 25 % chance level (one sample t-test for % time in target quadrant vs. chance level $p < 0.01$ for both groups; Figure 4C). At 120 hours of delay (probe 2), however, the preference for the target quadrant was intact for mice injected with control MoMulV, but was lost for mice injected with NL2A-MoMulV (two-way repeated measure ANOVA, main effect of % time in quadrant $F(3,81)=9.97$, $p < 0.0001$, Bonferroni post-tests target quadrant vs. opposite GFP $p < 0.01$ NL2A $p > 0.05$, target vs left quadrant GFP $p < 0.01$ NL2A $p > 0.05$, target vs right quadrant GFP $p < 0.001$ NL2A $p > 0.05$; one sample t-test for % time in target quadrant vs. chance level GFP $p < 0.01$, NL2A $p > 0.05$; Figure 4D). Thus, NL2A overexpression in newborn neurons impaired the retention of spatial memory at 120 hours delay.

Discussion

Here, we examined the effects of the cell-autonomous overexpression of different synaptic adhesion molecules on the development, synaptic integration and survival of newborn neurons in the hippocampus of 7- to 9-week-old mice. We found that adhesion molecules enhanced distinct aspects of new neurons' integration into the neuronal network. In particular, SynCAM1 increased the size and thus the morphological maturation of dendritic spines and MFT, while NL1B increased spine density. Although significant, the effects of SynCAM1 and NL1B overexpression on the synaptogenesis of newborn neurons were small in amplitude and did not increase neuronal survival. In contrast, NL2A overexpression increased both dendritic spine maturation and density, as well as GABAergic innervation and led to a robust increase in newborn neuron survival. These effects of synaptic adhesion molecules on new neurons support the idea of a competitive integration of newborn neurons in the neuronal network. Surprisingly, despite enhanced new neuron survival and integration, mice with newborn neurons overexpressing NL2A showed impaired memory performances in a Morris Water maze task. Together, these results indicate that overexpression of synaptic adhesion molecules can enhance the synaptic integration of new neurons in pre-existing neuronal networks, as well as their survival, but interfere with their functional integration. This is the first report showing that an increase in adult neurogenesis results in the impairment of memory retention of events that occurred subsequently to the manipulations of adult neurogenesis.

The effects of SynCAM1, NL1B or NL2A on synapse formation on new granule neurons are consistent with previously-described roles in other models of synaptogenesis. Indeed, in a comparative study, Sara et al. (Sara Y et al. 2005) showed that SynCAM1 but neither its cytosolic tail, nor NL1 increased synaptic efficacy in cultured hippocampal neurons, whereas only NL1 increased synapse number (Kwon HB *et al.* 2012). *In vivo*, the overexpression of

SynCAM1 in forebrain neurons increased the number of dendritic spines, and especially of mushroom spines (Robbins EM *et al.* 2010) and also increased presynaptic terminal formation (Biederer T *et al.* 2002; Fogel AI *et al.* 2007; Robbins EM *et al.* 2010). The splice variants of neuroligin demonstrate distinct properties and whereas NL1B overexpression increases glutamatergic puncta, NL2A overexpression increases the number of both glutamatergic and GABAergic puncta (Chih B *et al.* 2006). On new neurons in the adult hippocampus, the cell-autonomous overexpression of the splice variant NL1 increases spine density and the synaptic AMPA/NMDA excitatory post-synaptic current ratio (Schnell E *et al.* 2012). Similarly, the global overexpression of SynCAM1 in tetracycline-controlled transgenic mice increased spine density and volume of dendritic spines, as well as the survival of newborn neurons (Doengi M *et al.* 2015). Thus, our results are consistent with the notion that, *in vivo*, adhesion molecules play a role in synaptogenesis in the adult brain and contribute to the regulation of synaptic integration of new neurons. Furthermore, they support the hypothesis that the formation of synapses on new hippocampal neurons regulates their survival.

Although the effect of a decrease in adult neurogenesis does not necessarily lead to a decrease in memory performances (Jaholkowski P *et al.* 2009; Groves JO *et al.* 2013; Lazic SE *et al.* 2014), several lines of evidence indicate that an increase in adult neurogenesis results in improved performances in spatial memory tasks, such as in the Morris water maze (reviewed in (Zhao C *et al.* 2008; Deng W *et al.* 2010; Ming GL and H Song 2011)). Notably, directing fate progression of hippocampal progenitors towards neuronal progeny by the cell-specific overexpression of the pro-neurogenic transcription factor Neuro-D1, restored the delayed development of dendritic spines and the reduced survival of newborn neurons mouse model of Alzheimer's disease and resulted in increased performances in a spatial memory test (Richetin K *et al.* 2015). The role of new neurons in the formation of memory traces was further substantiated by the optogenetic silencing of their activity in mice undergoing a water maze

test, which resulted in impaired platform location (Gu Y *et al.* 2012). Recent results however challenged the notion that increased neurogenesis results in improved memory performance (Akers KG *et al.* 2014). Indeed, in their study, Akers *et al.* showed that an increase in adult neurogenesis occurring after a learned event induces its forgetting. However, the inverted experimental design of Akers *et al.* tested the persistence of memories acquired before the increase in neurogenesis and is therefore not comparable to our experimental design. In view of these results, we therefore expected that mice with NL2A-induced increase in neurogenesis would express enhanced memory performances. The apparent discrepancy between these previous results and our observations may be viewed in the light of the mechanisms of synaptic integration of newborn neurons. In particular, we consider two possibilities:

The first possibility is that synaptic adhesion molecules may interfere with the synaptic plasticity of newborn neurons. Indeed, immature neurons display increased LTP expression at around 4 weeks after division, a developmental stage at which their involvement in mechanisms of learning is the greatest (Schmidt-Hieber C *et al.* 2004; Gu Y *et al.* 2012). LTP requires structural plasticity of synapses, a mechanism that may be hindered by inter-cellular adhesion. Indeed, the overexpression of proteases increases LTP expression and memory performances (Madani R *et al.* 1999). Inversely, the overexpression of NL1 (Dahlhaus R *et al.* 2010), SynCAM1 (Robbins EM *et al.* 2010) or the manipulation of alternative splicing of Neurexin 3 (Aoto J *et al.* 2013) reduce synaptic plasticity. In view of these recent observations, it is possible that NL2A overexpression may inhibit the synaptic remodeling necessary for the expression of LTP or LTD and therefore reduce the plasticity of newborn neurons. However, the increased Arc expression in NL2A-overexpressing new neurons argues against impaired synaptic plasticity in these cells.

The second possibility is that NL2A overexpression in new neurons induces synapse formation with inappropriate presynaptic partners, which would otherwise not have been

contacted. The expression of the immediate-early gene *Arc* upon exposure to enriched environment in NL2A-overexpressing newborn neurons indicates that these cells are functionally integrated into the hippocampal network. However, input specificity may be impaired. Indeed, we have recently observed that any given nascent dendritic spine from a new neuron is surrounded, and touches, on average 5 presynaptic boutons with which a synaptic contact can potentially be formed (Krzisch M et al. 2015). It is believed that the connectivity between a given spine and its presynaptic bouton follows specific cues that are relevant to network activity occurring during the establishment of this connectivity (Bergami M and B Berninger 2012). Although not tested here, it is possible that such cues may be overridden by the over-expression of synaptic adhesion molecules and lead to lower input specificity of NL2A-overexpressing neurons. This possibility is consistent with the increased *Arc* expression in NL2A-overexpressing as compared to wild-type newborn neurons, indicating that a given stimulus will preferentially recruit NL2A-overexpressing new neurons. Recent work suggested that the alternative splicing of synaptic adhesion molecules may be a key mechanism for regulating neuronal recognition (Aoto J *et al.* 2013; Takahashi H and AM Craig 2013; Lah GJ et al. 2014). In particular, alternative splicing of neuroligins, the major ligand for neuroligins, produce over 1,000 isoforms, some of which are restricted to specific subtypes of neurons (Schreiner D et al. 2014). In this conceptual framework, the overexpression of NL2A in new neurons may interfere with synaptic identity and result in the formation of non-coherent networks, thereby disturbing the normal function of hippocampal network and its plasticity.

The synaptic integration of new neurons occurs simultaneously to the activity-dependent elimination of the majority of these cells. Although the mechanisms involved in the regulation, and the role of this selective elimination, remain unknown, the results presented

here suggest that the specificity of connectivity is required for the proper function of new neurons. Since several adhesion molecules are mutated in psychiatric disorders, the subsequent impaired functional integration of new neurons may contribute to the impaired cognitive function associated with these pathologies.

Funding

This work was supported by Swiss National Science Foundation (M.K., C.F., J.A., L.J., E.G., S.H., A.V., J.P.H., N.T), and by the Leenaards and Synapsis Foundations (N.T.).

Acknowledgements

The authors wish to thank Alejandro Schinder and Frédérique Varoqueaux for their insightful comments on this study, the precious contributions of Peter Scheiffele for kindly sharing the plasmid constructs for NL1B and NL2A, and of Thomas Biederer for kindly sharing the plasmid constructs for SynCAM and ctSynCAM, the Cellular Imaging Facility of the University of Lausanne for help with imaging and image analysis and Rudolf Kraftsik for help with statistical analysis.

References

- Akers KG, Martinez-Canabal A, Restivo L, Yiu AP, De Cristofaro A, Hsiang HL, Wheeler AL, Guskjolen A, Niibori Y, Shoji H, Ohira K, Richards BA, Miyakawa T, Josselyn SA, Frankland PW. 2014. Hippocampal neurogenesis regulates forgetting during adulthood and infancy. *Science* 344:598-602.
- Altman J, Das GD. 1965. Autoradiographic and histological evidence of postnatal hippocampal neurogenesis in rats. *J Comp Neurol* 124:319-335.
- Aoto J, Martinelli DC, Malenka RC, Tabuchi K, Sudhof TC. 2013. Presynaptic neurexin-3 alternative splicing trans-synaptically controls postsynaptic AMPA receptor trafficking. *Cell* 154:75-88.
- Bergami M, Berninger B. 2012. A fight for survival: the challenges faced by a newborn neuron integrating in the adult hippocampus. *Developmental neurobiology* 72:1016-1031.
- Biederer T, Sara Y, Mozhayeva M, Atasoy D, Liu X, Kavalali ET, Sudhof TC. 2002. SynCAM, a synaptic adhesion molecule that drives synapse assembly. *Science* 297:1525-1531.
- Biederer T, Stagi M. 2008. Signaling by synaptogenic molecules. *Current opinion in neurobiology* 18:261-269.

Boucard AA, Chubykin AA, Comoletti D, Taylor P, Sudhof TC. 2005. A splice code for trans-synaptic cell adhesion mediated by binding of neuroligin 1 to alpha- and beta-neurexins. *Neuron* 48:229-236.

Brus M, Keller M, Levy F. 2013. Temporal features of adult neurogenesis: differences and similarities across mammalian species. *Frontiers in neuroscience* 7:135.

Budreck EC, Kwon OB, Jung JH, Baudouin S, Thommen A, Kim HS, Fukazawa Y, Harada H, Tabuchi K, Shigemoto R, Scheiffele P, Kim JH. 2013. Neuroligin-1 controls synaptic abundance of NMDA-type glutamate receptors through extracellular coupling. *Proc Natl Acad Sci U S A* 110:725-730.

Chancey JH, Adlaf EW, Sapp MC, Pugh PC, Wadiche JI, Overstreet-Wadiche LS. 2013. GABA depolarization is required for experience-dependent synapse unsilencing in adult-born neurons. *J Neurosci* 33:6614-6622.

Chih B, Engelman H, Scheiffele P. 2005. Control of excitatory and inhibitory synapse formation by neuroligins. *Science* 307:1324-1328.

Chih B, Gollan L, Scheiffele P. 2006. Alternative splicing controls selective trans-synaptic interactions of the neuroligin-neurexin complex. *Neuron* 51:171-178.

Comoletti D, Flynn RE, Boucard AA, Demeler B, Schirf V, Shi J, Jennings LL, Newlin HR, Sudhof TC, Taylor P. 2006. Gene selection, alternative splicing, and post-translational processing regulate neuroligin selectivity for beta-neurexins. *Biochemistry* 45:12816-12827.

Craig AM, Kang Y. 2007. Neurexin-neuroligin signaling in synapse development. *Current opinion in neurobiology* 17:43-52.

Dahlhaus R, Hines RM, Eadie BD, Kannangara TS, Hines DJ, Brown CE, Christie BR, El-Husseini A. 2010. Overexpression of the cell adhesion protein neuroligin-1 induces learning deficits and impairs synaptic plasticity by altering the ratio of excitation to inhibition in the hippocampus. *Hippocampus* 20:305-322.

Deng W, Aimone JB, Gage FH. 2010. New neurons and new memories: how does adult hippocampal neurogenesis affect learning and memory? *Nat Rev Neurosci* 11:339-350.

Deng W, Saxe MD, Gallina IS, Gage FH. 2009. Adult-born hippocampal dentate granule cells undergoing maturation modulate learning and memory in the brain. *J Neurosci* 29:13532-13542.

Doengi M, Krupp AJ, Korber N, Stein V. 2015. SynCAM 1 improves survival of adult-born neurons by accelerating synapse maturation. *Hippocampus*.

Eriksson PS, Perfilieva E, Bjork-Eriksson T, Alborn AM, Nordborg C, Peterson DA, Gage FH. 1998. Neurogenesis in the adult human hippocampus. *Nat Med* 4:1313-1317.

Fogel AI, Akins MR, Krupp AJ, Stagi M, Stein V, Biederer T. 2007. SynCAMs organize synapses through heterophilic adhesion. *J Neurosci* 27:12516-12530.

Ge S, Goh EL, Sailor KA, Kitabatake Y, Ming GL, Song H. 2006. GABA regulates synaptic integration of newly generated neurons in the adult brain. *Nature* 439:589-593.

Ge S, Yang CH, Hsu KS, Ming GL, Song H. 2007. A critical period for enhanced synaptic plasticity in newly generated neurons of the adult brain. *Neuron* 54:559-566.

Giagtzoglou N, Ly CV, Bellen HJ. 2009. Cell adhesion, the backbone of the synapse: "vertebrate" and "invertebrate" perspectives. *Cold Spring Harbor perspectives in biology* 1:a003079.

Graf ER, Zhang X, Jin SX, Linhoff MW, Craig AM. 2004. Neurexins induce differentiation of GABA and glutamate postsynaptic specializations via neuroligins. *Cell* 119:1013-1026.

Groves JO, Leslie I, Huang GJ, McHugh SB, Taylor A, Mott R, Munafo M, Bannerman DM, Flint J. 2013. Ablating adult neurogenesis in the rat has no effect on spatial processing: evidence from a novel pharmacogenetic model. *PLoS Genet* 9:e1003718.

Gu Y, Arruda-Carvalho M, Wang J, Janoschka SR, Josselyn SA, Frankland PW, Ge S. 2012. Optical controlling reveals time-dependent roles for adult-born dentate granule cells. *Nature neuroscience* 15:1700-1706.

Hauser T, Klaus F, Lipp HP, Amrein I. 2009. No effect of running and laboratory housing on adult hippocampal neurogenesis in wild caught long-tailed wood mouse. *BMC neuroscience* 10:43.

Henn FA, Vollmayr B. 2004. Neurogenesis and depression: etiology or epiphenomenon? *Biological psychiatry* 56:146-150.

Hoon M, Soykan T, Falkenburger B, Hammer M, Patrizi A, Schmidt KF, Sassoe-Pognetto M, Lowel S, Moser T, Taschenberger H, Brose N, Varoqueaux F. 2011. Neuroligin-4 is localized to glycinergic postsynapses and regulates inhibition in the retina. *Proc Natl Acad Sci U S A* 108:3053-3058.

Ichtchenko K, Hata Y, Nguyen T, Ullrich B, Missler M, Moomaw C, Sudhof TC. 1995. Neuroligin 1: a splice site-specific ligand for beta-neurexins. *Cell* 81:435-443.

Jaholkowski P, Kiryk A, Jedynek P, Ben Abdallah NM, Knapska E, Kowalczyk A, Piechal A, Blecharz-Klin K, Figiel I, Liudyno V, Widy-Tyszkiewicz E, Wilczynski GM, Lipp HP, Kaczmarek L, Filipkowski RK. 2009. New hippocampal neurons are not obligatory for memory formation; cyclin D2 knockout mice with no adult brain neurogenesis show learning. *Learning & memory* 16:439-451.

Jin Y, Garner CC. 2008. Molecular mechanisms of presynaptic differentiation. *Annual review of cell and developmental biology* 24:237-262.

Kempermann G, Gast D, Kronenberg G, Yamaguchi M, Gage FH. 2003. Early determination and long-term persistence of adult-generated new neurons in the hippocampus of mice. *Development* 130:391-399.

Kempermann G, Kuhn HG, Gage FH. 1997. More hippocampal neurons in adult mice living in an enriched environment. *Nature* 386:493-495.

Kohler SJ, Williams NI, Stanton GB, Cameron JL, Greenough WT. 2011. Maturation time of new granule cells in the dentate gyrus of adult macaque monkeys exceeds six months. *Proc Natl Acad Sci U S A* 108:10326-10331.

Krzisch M, Sultan S, Sandell J, Demeter K, Vutskits L, Toni N. 2013. Propofol anesthesia impairs the maturation and survival of adult-born hippocampal neurons. *Anesthesiology* 118:602-610.

Krzisch M, Temprana SG, Mongiat LA, Armida J, Schmutz V, Virtanen MA, Kocher-Braissant J, Kraftsik R, Vutskits L, Conzelmann KK, Bergami M, Gage FH, Schinder AF, Toni N. 2015. Pre-existing astrocytes form functional perisynaptic processes on neurons generated in the adult hippocampus. *Brain Struct Funct* 220:2027-2042.

Kwon HB, Kozorovitskiy Y, Oh WJ, Peixoto RT, Akhtar N, Saulnier JL, Gu C, Sabatini BL. 2012. Neuroligin-1-dependent competition regulates cortical synaptogenesis and synapse number. *Nature neuroscience* 15:1667-1674.

Lah GJ, Li JS, Millard SS. 2014. Cell-specific alternative splicing of *Drosophila Dscam2* is crucial for proper neuronal wiring. *Neuron* 83:1376-1388.

Lazic SE, Fuss J, Gass P. 2014. Quantifying the behavioural relevance of hippocampal neurogenesis. *PLoS One* 9:e113855.

Madani R, Hulo S, Toni N, Madani H, Steimer T, Muller D, Vassalli JD. 1999. Enhanced hippocampal long-term potentiation and learning by increased neuronal expression of tissue-type plasminogen activator in transgenic mice. *The EMBO journal* 18:3007-3012.

Marin-Burgin A, Mongiat LA, Pardi MB, Schinder AF. 2012. Unique processing during a period of high excitation/inhibition balance in adult-born neurons. *Science* 335:1238-1242.

Matsuzaki M, Ellis-Davies GC, Nemoto T, Miyashita Y, Iino M, Kasai H. 2001. Dendritic spine geometry is critical for AMPA receptor expression in hippocampal CA1 pyramidal neurons. *Nature neuroscience* 4:1086-1092.

Ming GL, Song H. 2011. Adult neurogenesis in the mammalian brain: significant answers and significant questions. *Neuron* 70:687-702.

Nguyen T, Sudhof TC. 1997. Binding properties of neuroligin 1 and neurexin 1beta reveal function as heterophilic cell adhesion molecules. *The Journal of biological chemistry* 272:26032-26039.

Prange O, Wong TP, Gerrow K, Wang YT, El-Husseini A. 2004. A balance between excitatory and inhibitory synapses is controlled by PSD-95 and neuroligin. *Proc Natl Acad Sci U S A* 101:13915-13920.

Richetin K, Leclerc C, Toni N, Gallopin T, Pech S, Roybon L, Rampon C. 2015. Genetic manipulation of adult-born hippocampal neurons rescues memory in a mouse model of Alzheimer's disease. *Brain : a journal of neurology* 138:440-455.

Robbins EM, Krupp AJ, Perez de Arce K, Ghosh AK, Fogel AI, Boucard A, Sudhof TC, Stein V, Biederer T. 2010. SynCAM 1 adhesion dynamically regulates synapse number and impacts plasticity and learning. *Neuron* 68:894-906.

Sahay A, Scobie KN, Hill AS, O'Carroll CM, Kheirbek MA, Burghardt NS, Fenton AA, Dranovsky A, Hen R. 2011. Increasing adult hippocampal neurogenesis is sufficient to improve pattern separation. *Nature* 472:466-470.

Sara Y, Biederer T, Atasoy D, Chubykin A, Mozhayeva MG, Sudhof TC, Kavalali ET. 2005. Selective capability of SynCAM and neuroligin for functional synapse assembly. *J Neurosci* 25:260-270.

Saxe MD, Battaglia F, Wang JW, Malleret G, David DJ, Monckton JE, Garcia AD, Sofroniew MV, Kandel ER, Santarelli L, Hen R, Drew MR. 2006. Ablation of hippocampal neurogenesis impairs contextual fear conditioning and synaptic plasticity in the dentate gyrus. *Proc Natl Acad Sci U S A* 103:17501-17506.

Scheiffele P, Fan J, Choih J, Fetter R, Serafini T. 2000. Neuroligin expressed in nonneuronal cells triggers presynaptic development in contacting axons. *Cell* 101:657-669.

Schmidt-Hieber C, Jonas P, Bischofberger J. 2004. Enhanced synaptic plasticity in newly generated granule cells of the adult hippocampus. *Nature* 429:184-187.

Schnell E, Bensen AL, Washburn EK, Westbrook GL. 2012. Neuroligin-1 overexpression in newborn granule cells in vivo. *PLoS One* 7:e48045.

Schreiner D, Nguyen TM, Russo G, Heber S, Patrignani A, Ahrne E, Scheiffele P. 2014. Targeted combinatorial alternative splicing generates brain region-specific repertoires of neurexins. *Neuron* 84:386-398.

Song J, Sun J, Moss J, Wen Z, Sun GJ, Hsu D, Zhong C, Davoudi H, Christian KM, Toni N, Ming GL, Song H. 2013. Parvalbumin interneurons mediate neuronal circuitry-neurogenesis coupling in the adult hippocampus. *Nature neuroscience* 16:1728-1730.

Song JY, Ichtchenko K, Sudhof TC, Brose N. 1999. Neuroligin 1 is a postsynaptic cell-adhesion molecule of excitatory synapses. *Proc Natl Acad Sci U S A* 96:1100-1105.

Sultan S, Gebara E, Toni N. 2013. Doxycycline increases neurogenesis and reduces microglia in the adult hippocampus. *Frontiers in neuroscience* 7:131.

Sultan S, Li L, Moss J, Petrelli F, Casse F, Gebara E, Lopatar J, Pfrieger FW, Bezzi P, Bischofberger J, Toni N. 2015. Synaptic Integration of Adult-Born Hippocampal Neurons Is Locally Controlled by Astrocytes. *Neuron*.

Takahashi H, Craig AM. 2013. Protein tyrosine phosphatases PTPdelta, PTPsigma, and LAR: presynaptic hubs for synapse organization. *Trends in neurosciences* 36:522-534.

Takumi Y, Ramirez-Leon V, Laake P, Rinvik E, Ottersen OP. 1999. Different modes of expression of AMPA and NMDA receptors in hippocampal synapses. *Nature neuroscience* 2:618-624.

Tashiro A, Makino H, Gage FH. 2007. Experience-specific functional modification of the dentate gyrus through adult neurogenesis: a critical period during an immature stage. *J Neurosci* 27:3252-3259.

Tashiro A, Sandler VM, Toni N, Zhao C, Gage FH. 2006. NMDA-receptor-mediated, cell-specific integration of new neurons in adult dentate gyrus. *Nature* 442:929-933.

Toni N, Laplagne DA, Zhao C, Lombardi G, Ribak CE, Gage FH, Schinder AF. 2008. Neurons born in the adult dentate gyrus form functional synapses with target cells. *Nature neuroscience* 11:901-907.

Toni N, Sultan S. 2011. Synapse formation on adult-born hippocampal neurons. *The European journal of neuroscience* 33:1062-1068.

Toni N, Teng EM, Bushong EA, Aimone JB, Zhao C, Consiglio A, van Praag H, Martone ME, Ellisman MH, Gage FH. 2007. Synapse formation on neurons born in the adult hippocampus. *Nature neuroscience* 10:727-734.

Tozuka Y, Fukuda S, Namba T, Seki T, Hisatsune T. 2005. GABAergic excitation promotes neuronal differentiation in adult hippocampal progenitor cells. *Neuron* 47:803-815.

Tronel S, Fabre A, Charrier V, Oliet SH, Gage FH, Abrous DN. 2010. Spatial learning sculpts the dendritic arbor of adult-born hippocampal neurons. *Proc Natl Acad Sci U S A* 107:7963-7968.

van Praag H, Christie BR, Sejnowski TJ, Gage FH. 1999. Running enhances neurogenesis, learning, and long-term potentiation in mice. *Proc Natl Acad Sci U S A* 96:13427-13431.

Varoqueaux F, Aramuni G, Rawson RL, Mohrmann R, Missler M, Gottmann K, Zhang W, Sudhof TC, Brose N. 2006. Neuroligins determine synapse maturation and function. *Neuron* 51:741-754.

Varoqueaux F, Jamain S, Brose N. 2004. Neuroligin 2 is exclusively localized to inhibitory synapses. *European journal of cell biology* 83:449-456.

Zeidan A, Ziv NE. 2012. Neuroligin-1 loss is associated with reduced tenacity of excitatory synapses. *PLoS One* 7:e42314.

Zhao C, Deng W, Gage FH. 2008. Mechanisms and functional implications of adult neurogenesis. *Cell* 132:645-660.

Zhao C, Teng EM, Summers RG, Jr., Ming GL, Gage FH. 2006. Distinct morphological stages of dentate granule neuron maturation in the adult mouse hippocampus. *J Neurosci* 26:3-11.

Figure legends

Figure 1: Effect of ctSynCAM1 and SynCAM1 overexpression on newborn neurons maturation and survival

A. Left panel: experimental timeline and schematic procedure for *in vivo* gene delivery: The dentate gyrus of 7- to 9-week-old mice was injected with a mix of two retroviruses, one carrying the expression cassette of the gene of interest, and the other one carrying the control construct. Animals were sacrificed at 14, 21 or 28 dpi and new neurons' morphology and survival was analyzed. Right panel: Illustration of a granule neuron in the granule cell layer (GCL), projecting dendrites in the ML. **B-C.** Density of dendritic protrusions of control

(white), SynCAM1-overexpressing (grey) and ctSynCAM1-overexpressing (black) newborn neurons in the first third (**B**) and second third (**C**) of the ML. **D**. Confocal maximal intensity projection of a dendrite, illustrating the three classes of dendritic protrusions: filopodia (F), thin (T) and mushroom spines (M). **E-F**. Proportion of protrusions with filopodia, thin or mushroom morphologies in ctSynCAM1-expressing neurons at 21 (**E**) and 28 dpi (**F**). **G-H**. Proportion of filopodia, thin and mushroom spines in control and SynCAM1-overexpressing neurons at 21 (**G**) and 28 dpi (**H**). **I**. Confocal maximal intensity projections of representative MFT for each group at 28 dpi. **J**. Schematic illustration of the perimeter, projection area, circularity and number of extensions on MFT. **K-N**. Mean area (**K**), perimeter (**L**), circularity (**M**) and number of extensions (**N**) on MFT. **O**. Schematic illustration of the relative quantification of survival of transgenic and control neurons. **P**. Average ratio of the total number of ctSynCAM1-expressing neurons and the total number of control neurons per mouse. **Q**. Average ratio of the total number of SynCAM1-overexpressing neurons and the total number of control neurons per mouse. dpi: days post-injection; *: $p < 0.05$; **: $p < 0.01$; ***: $p < 0.001$. Scale bars: $5\mu\text{m}$ (**D**) and 10 m (**I**).

Figure 2: Effect of NL1B overexpression on new neurons

A. Confocal maximal projections of dendrites from control or NL1B-overexpressing newborn neurons at 28 dpi. Scale bar: $2\mu\text{m}$. **B-C**. Density of dendritic protrusions of control and NL1B-overexpressing newborn neurons in the first third (**B**) and the second third of the ML (**C**). **D-E**. Percentage of filopodia, thin and mushroom spines in control and NL1B-overexpressing neurons at 21 (**D**) and 28 dpi (**E**). **F-I**. Mean area (**F**), perimeter (**G**), circularity (**H**) and number of extensions (**I**) on MFT at 28 dpi. **J**. Average ratio of the total number of NL1B-overexpressing neurons over the total number of control neurons per mouse at 14 and 28 dpi. *: $p < 0.05$

Figure 3: Effect of NL2A overexpression on new neurons

A-B. Density of dendritic protrusions of control and NL2A-overexpressing newborn neurons in the first third (**A**) and the second third of the ML (**B**). **C-D.** Percentage of filopodia, thin and mushroom spines in control and NL2A-overexpressing neurons at 21 (**C**) and 28 dpi (**D**). **E.** Representative confocal maximal intensity projections of dendritic segments of control and NL2A-overexpressing neurons in the first third of the ML at 28 dpi. Scale bar: 1 μ m. **F-I.** Mean area (**F**), perimeter (**G**) circularity (**H**) and number of extensions (**I**) on MFTs at 28 dpi. **J.** Representative confocal plans of new neurons at 21 dpi (red) in slices immunostained for VGAT (green) and GABA_A receptors (blue). Arrows point to GABAergic synapses, defined as appositions of GABAAR⁺ and VGAT⁺ puncta in soma (left panel) and dendritic segment (right panel). Scale bars: 5 μ m. **K-L.** Number of VGAT-positive and GABA_A receptor-positive puncta per soma (**K**) and primary dendritic segment (**L**) in control and NL2A-overexpressing neurons at 21 dpi. **M.** Average ratio between the total number of NL2A-overexpressing neurons and the total number of control neurons per mouse at 14 and 28 dpi. **N.** Percentage of cells expressing Arc in control and NL2A-overexpressing newborn neurons after environmental enrichment. *: p<0.05; **: p<0.01; ***: p<0.001;

Figure 4: NL2A overexpression in new neurons decreases memory performances at 40 dpi

A. Experimental timeline: Mice were injected with virus expressing NL2A or GFP (as control). At 24 dpi, mice were tested on an elevated plus maze. At 28 dpi, mice were trained on a water maze for 7 days (4 trials per day, MWM1). A first probe trial was run 24 hours later, followed by another trial at 120hours. **B.** Escape latency time during the water mazetraining. **C.** Time spent in each quadrant during the probe trial 24h after the last training

session. Bottom panels are heatmaps of all animals' trajectories during the probe trial. **D.** Time spent in each quadrant during the probe trial 120h after the last training session. Bottom panels are heatmaps of all animals' trajectories during the probe trial. *: $p < 0.05$

Supplementary Figure 1: Retroviral infection leads to the effective expression of adhesion molecules *in vitro*

A. Schematic representations of the retroviral constructs used in this study. **B.** Left panels: pictures of a single confocal plan from HEK 293T cells infected with the viruses carrying the different constructs. Right panels: plot profiles of the fluorescence intensity of the different markers along the white dashed lines shown on the pictures. Scale bars: 10 μm . **C.** Immunoblots showing immunoreactivities of GFP, RFP, ctSyncam1, Syncam1, NL1B and NL2A of total proteins extracted from HEK 293T cells transfected with the different constructs.

Supplementary Figure 2: Effect of SynCAM1, ctSynCAM1, NL1B and NL2A overexpression on the dendritic arborization of new neurons

A-D. Scholl analysis of the dendritic arborization of SynCAM1 (**A**), ctSynCAM1 (**B**), NL1B (**C**) and NL2A (**D**) -overexpressing and control neurons at 14, 21 and 28 dpi, as indicated. **: $p < 0.01$

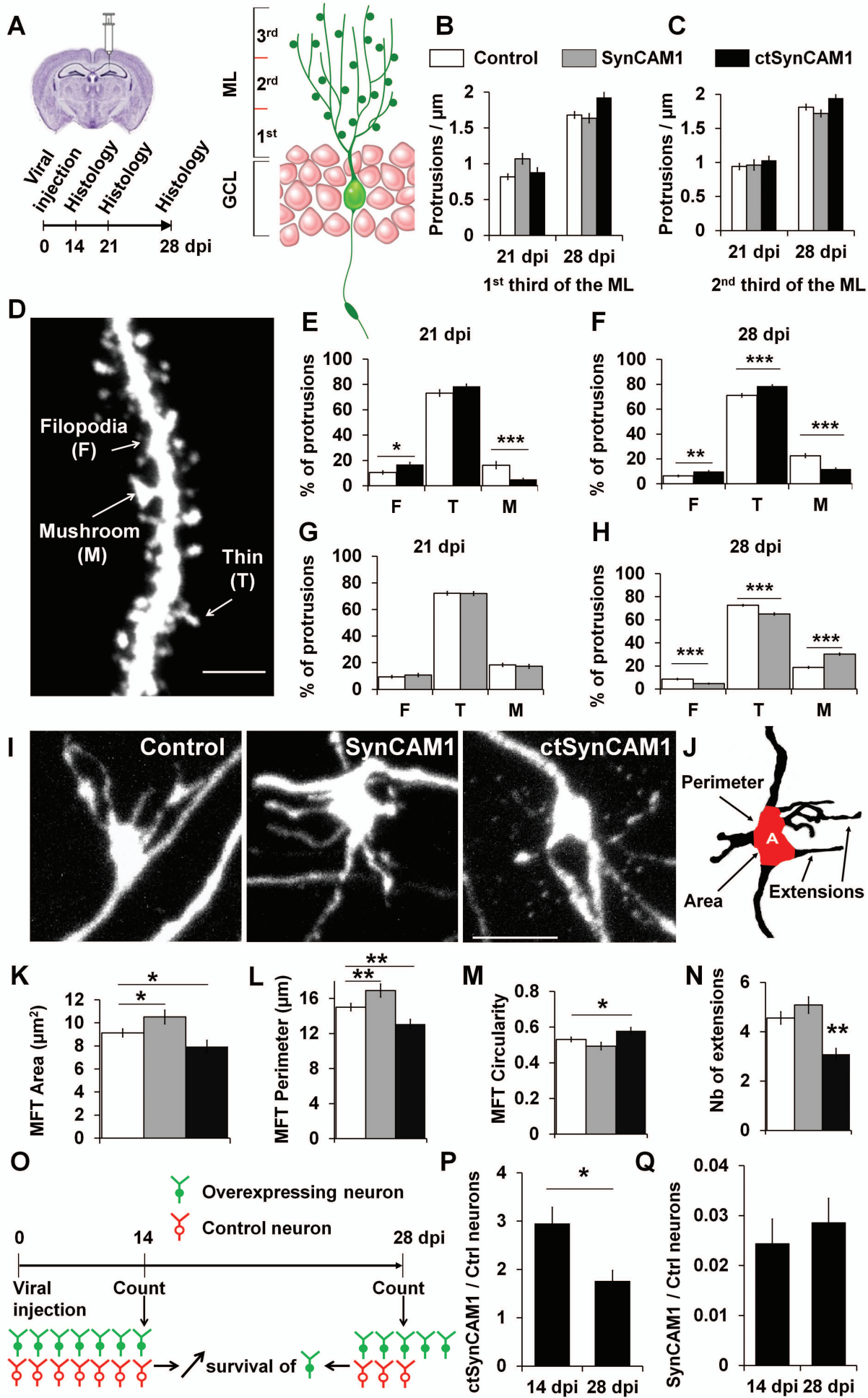
Fig. 1

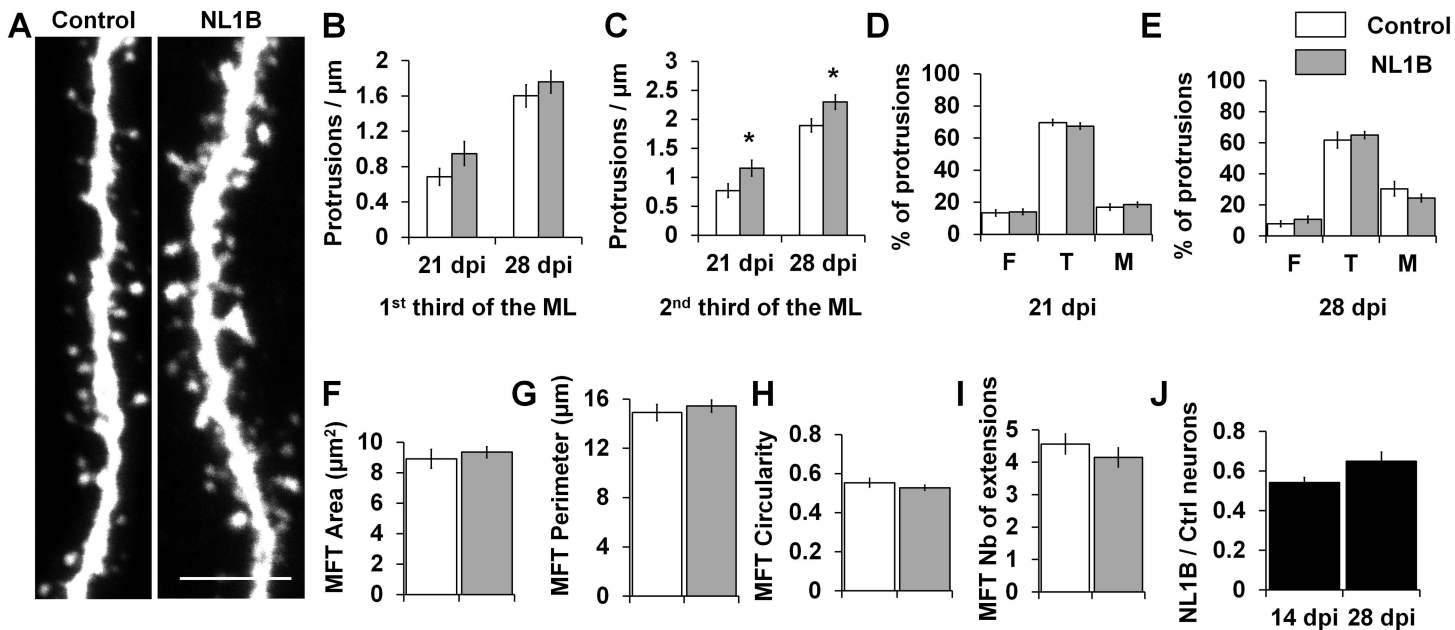
Fig. 2

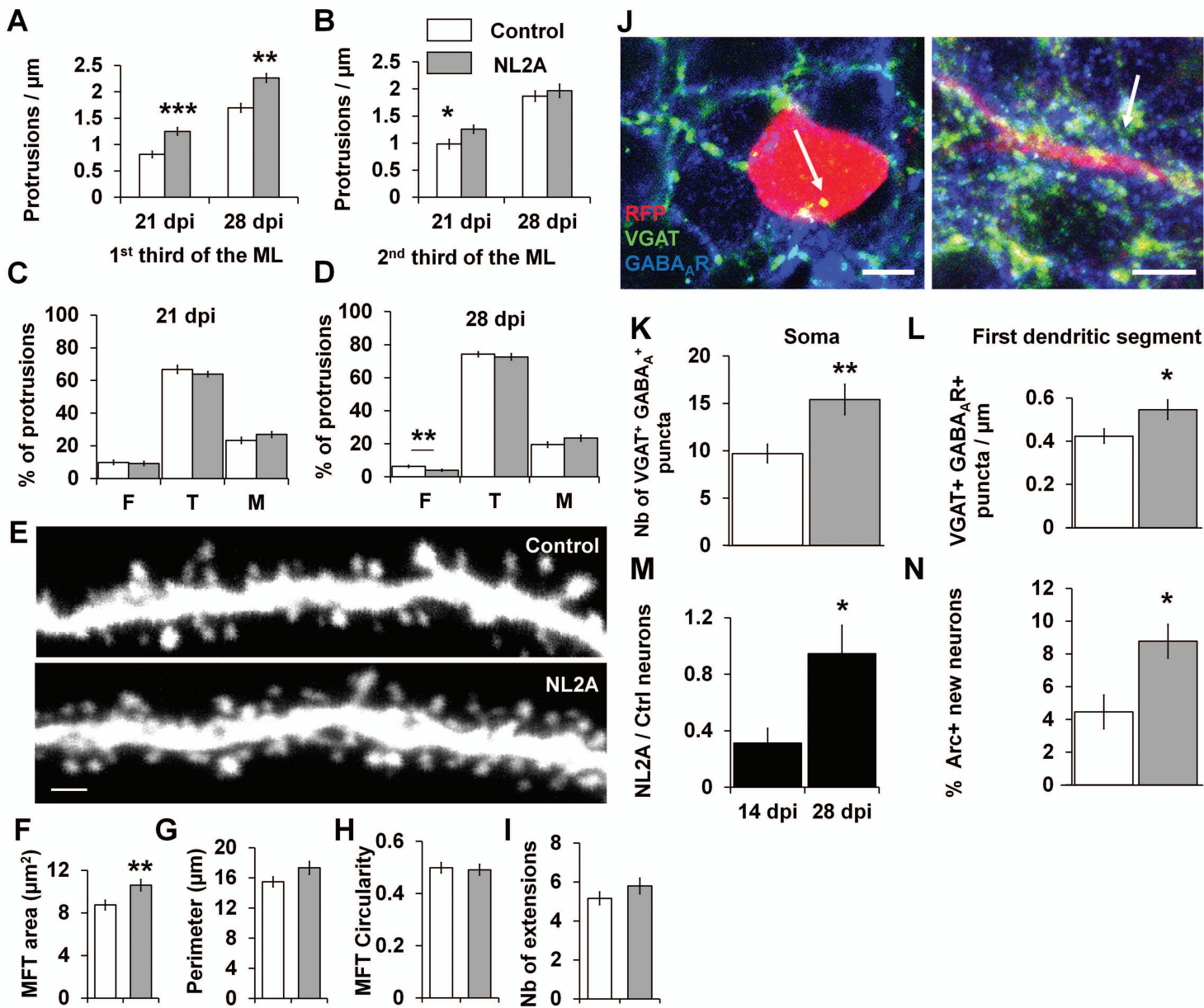
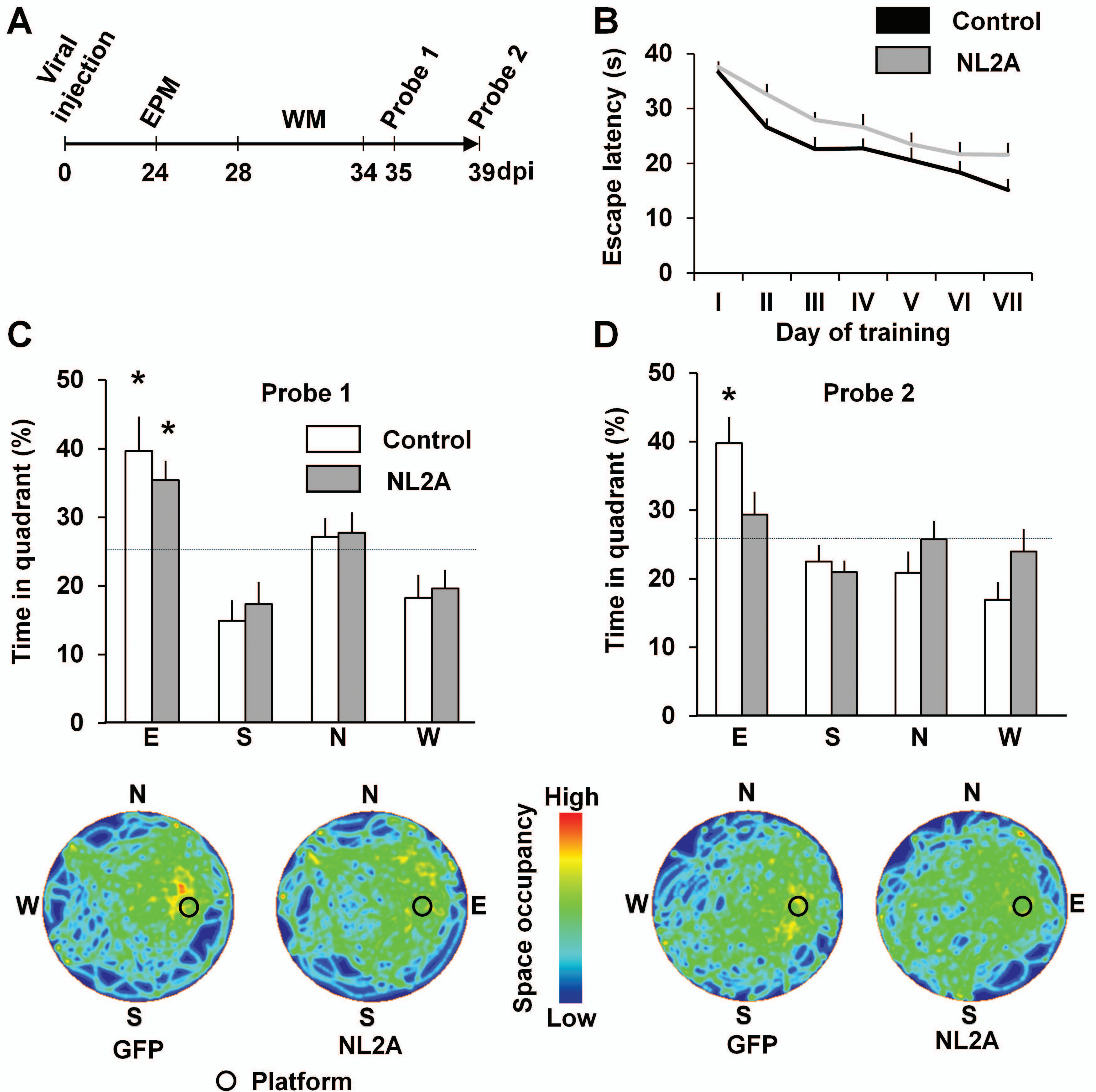
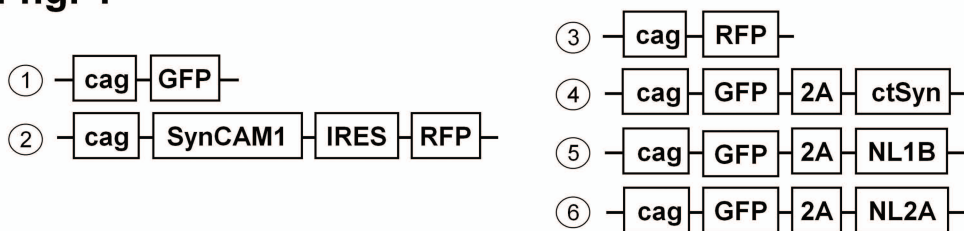
Fig. 3

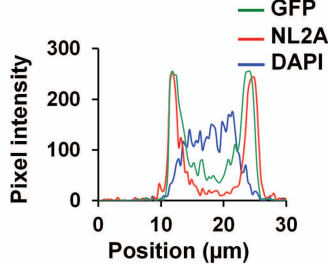
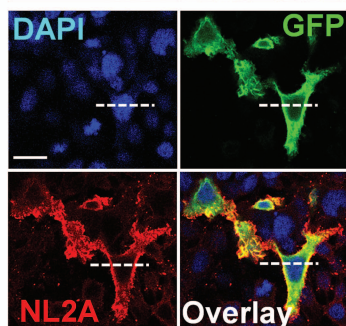
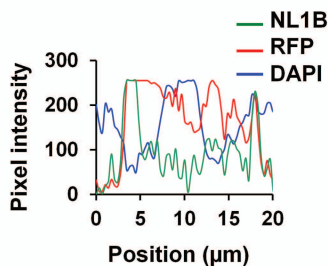
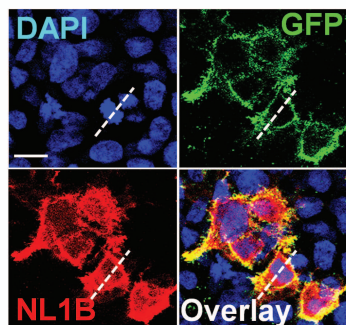
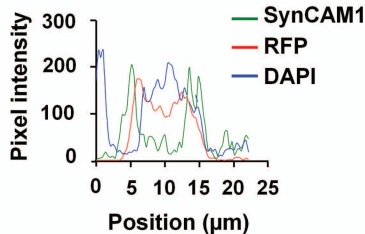
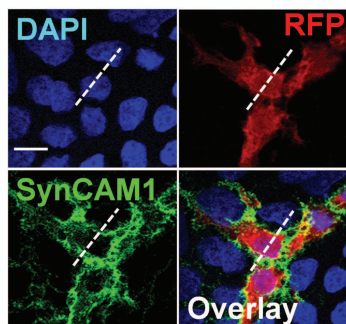
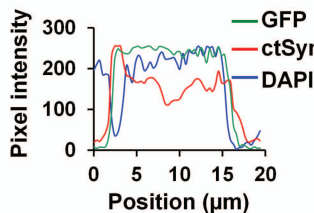
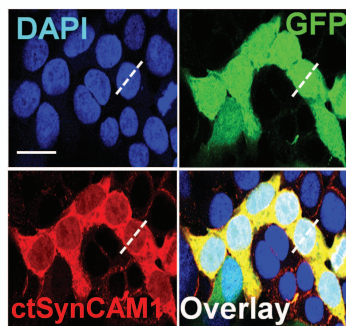
Fig. 4

Suppl. fig. 1

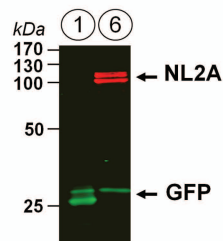
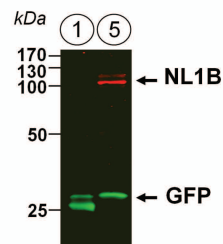
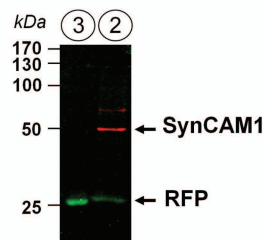
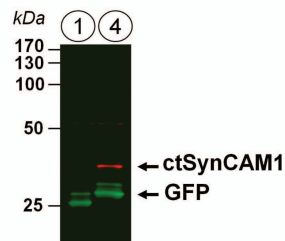
A



B

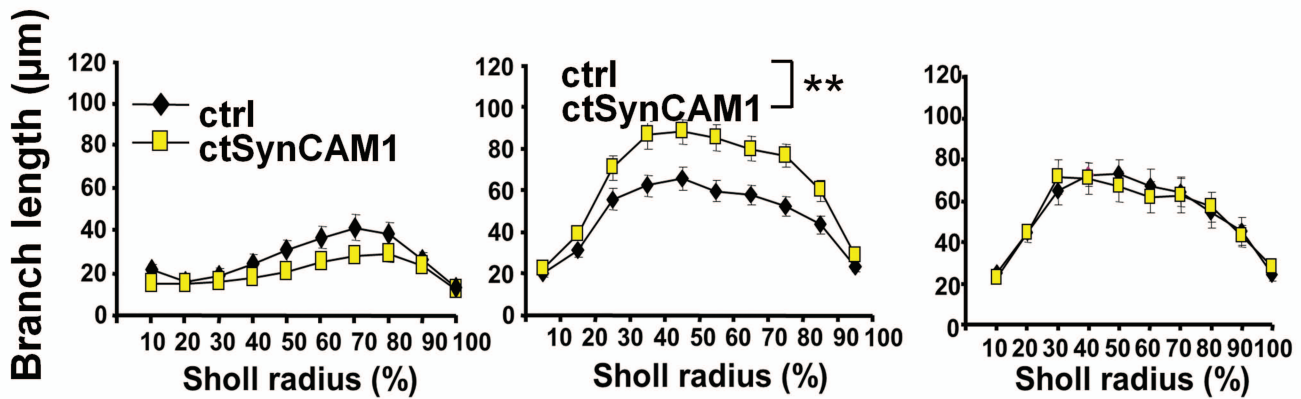


C

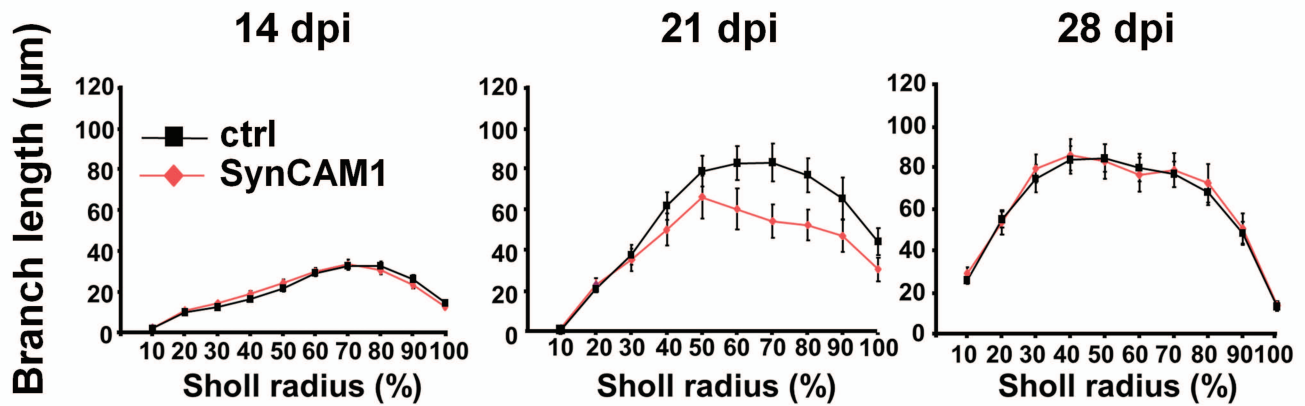


Suppl. fig. 2

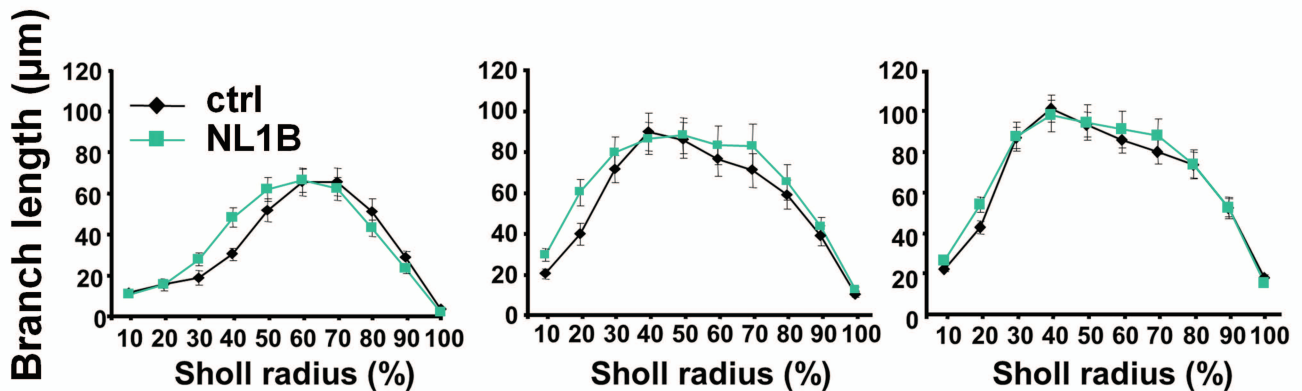
A



B



C



D

